



ÄSPÖLABORATORIET

**INTERNATIONAL
COOPERATION
REPORT**

94-04

**Design constraints and process
discrimination for the Detailed Scale
Tracer Experiments at Äspö -
Multiple Well Tracer Experiment and
Matrix Diffusion**

Jan-Olof Selroos¹, Anders Winberg², Vladimir Cvetkovic¹

¹ Water Resources Eng., KTH

² Conterra AB

April 1994

Supported by SKB, Sweden

102.8

SVENSK KÄRNBRÄNSLEHANTERING AB
SWEDISH NUCLEAR FUEL AND WASTE MANAGEMENT CO

BOX 5864 S-102 40 STOCKHOLM

TEL. +46-8-665 28 00 TELEX 13108 SKB TELEFAX +46-8-661 57 19

9505040345 950424
PDR WASTE PDR
WM-11

*Rec'd with file
NO 4/25/95*

DESIGN CONSTRAINTS AND PROCESS DISCRIMINATION FOR THE DETAILED SCALE TRACER EXPERIMENTS AT ÄSPÖ

MULTIPLE WELL TRACER EXPERIMENT AND MATRIX DIFFUSION EXPERIMENT

Jan-Olof Selroos¹, Anders Winberg²,
Vladimir Cvetkovic¹

1 Water Resources Eng., KTH
2 Conterra AB

April 1994

Supported by SKB, Sweden

This document concerns a study which was conducted within an Äspö HRL joint project. The conclusions and viewpoints expressed are those of the author(s) and do not necessarily coincide with those of the client(s). The supporting organization has reviewed the document according to their documentation procedure.

102.8

DESIGN CONSTRAINTS AND
PROCESS DISCRIMINATION FOR
THE DETAILED SCALE TRACER EXPERIMENTS
AT ÄSPÖ

MULTIPLE WELL TRACER EXPERIMENT

and

MATRIX DIFFUSION EXPERIMENT

Jan-Olof Selroos, Water Resources Eng., KTH
Anders Winberg, Conterra AB
Vladimir Cvetkovic, Water Resources Eng., KTH

April 1994

Keywords: Tracer experiments, transport models, identification of processes, rate-limited mass transfer, spatial variability in transmissivity.

ABSTRACT

Scoping calculations were performed of planned tracer experiments on a detailed scale at the Äspö Hard Rock Laboratory to investigate 1) under what experimental conditions various non-equilibrium (rate-limiting) mass transfer phenomena are identifiable; 2) to present design criteria for the planned Multiple Well Tracer Experiment (MWTE) and the Matrix Diffusion Experiment (MDE). A stochastic continuum methodology was used to model the spatially variable transmissivity field in the fracture plane whereupon the flow problem was solved using finite difference techniques in simulated flow fields. Solute transport was modelled with a particle tracking scheme assuming conservative solute particles. Using the conservative travel times, the rate-limiting mass transfer was incorporated using semi-analytical solution techniques. A matrix diffusion model combined with possible equilibrium sorption in the matrix and a general non-equilibrium sorption-desorption model were used for the MWTE. The results indicate that heterogeneity in transmissivity, rate-limiting mass transfer, and the assumed dipole flow field, all are manifested by tailing in solute arrival. Hence, it may be difficult to distinguish these processes. For the MDE a single injection well was considered, and the breakthrough was monitored at control surfaces encircling the well. Matrix diffusion combined with possible equilibrium sorption in the matrix are the only mass transfer processes considered. A specific objective of the MDE is to investigate the effect of spatial variability in transmissivity on the diffusion process and the resulting diffusion-affected breakthrough. The dependence of the calculated breakthroughs on pumping rate, travel distance and rate coefficient is in the case of matrix diffusion presented in a dimensionless form for given transmissivity statistics and boundary conditions. These nomograms can be used for detailed scopings once a fracture has been targeted.

TABLE OF CONTENTS

	page
SUMMARY	iii
1 BACKGROUND AND INTRODUCTION	1
1.1 RATIONALE BEHIND DETAILED SCALE EXPERIMENTS	1
1.2 DETAILED SCALE EXPERIMENTS IN PERSPECTIVE	2
1.3 SCOPE OF WORK PERFORMED	3
2 MATHEMATICAL DESCRIPTION	5
2.1 DIFFUSION MODEL	5
2.2 SORPTION MODEL	7
2.3 FLOW AND NONREACTIVE TRANSPORT MODELS	8
2.3.1 Homogeneous flow	8
2.3.2 Heterogeneous flow	9
2.3.3 Nonreactive transport	10
2.4 DIFFUSION CORRELATED WITH TRAVEL TIME	10
3 FRACTURE PROPERTY DATA	13
3.1 TRANSMISSIVITY AND APERTURE MEASUREMENTS	13
3.2 SPATIAL VARIABILITY OF HYDRAULIC PROPERTIES	14
3.3 FRACTURE PARAMETERS PERTINENT TO ÄSPÖ	15
4 MULTIPLE WELL TRACER EXPERIMENT	18
4.1 EXPERIMENTAL SETUP	18
4.2 DISCUSSION AND RESULTS	19
4.2.1 Matrix diffusion	19
4.2.2 Rate-limited surface sorption	24
4.3 CONCLUSIONS	25
5 MATRIX DIFFUSION EXPERIMENT	27
5.1 EXPERIMENTAL SETUP	27
5.2 DISCUSSION AND RESULTS	28
5.3 CONCLUSIONS	30

6	DESIGN CONSTRAINTS	32
6.1	MULTIPLE WELL TRACER EXPERIMENT	32
6.2	MATRIX DIFFUSION EXPERIMENT	33
7	REFERENCES	34
8	APPENDICES	37

Appendix 1: Condensed description of conceptual model components

SUMMARY

The results presented in this study are based on scoping calculations of planned tracer experiments on a detailed scale at the Äspö Hard Rock Laboratory. The objective of the study are 1) to investigate under what experimental conditions various non-equilibrium (rate-limiting) mass transfer phenomena are identifiable; 2) to present design criteria for the planned Multiple Well Tracer Experiment (MWTE) on a detailed scale and the Matrix Diffusion Experiment (MDE) based on the results obtained. A stochastic continuum methodology is used to model the spatially variable transmissivity field in the fracture plane. Using specified boundary conditions the flow problem is solved using a direct finite difference solver. Subsequently, solute transport is modelled using a particle tracking scheme where the solute particles are advected without being subject to molecular diffusion or local dispersion. The numerical model is verified by comparing results with an analytical solution for cases with homogeneous transmissivity. Having established the conservative travel times, the effect of rate-limiting mass transfer is incorporated using recently developed semi-analytical procedures. For the MWTE two different rate-limiting mass transfer models are considered; a matrix diffusion model combined with possible equilibrium sorption in the rock matrix and a general non-equilibrium sorption-desorption model describing the rate of accumulation and release from the immobile part of the system (e.g. stagnant water in dead-end pore spaces). In the matrix diffusion model an effective rate coefficient is related to the aperture, matrix porosity and matrix diffusion coefficient.

The results indicate that heterogeneity in transmissivity, rate-limiting mass transfer, and a dipole well configuration, are all manifested by tailing in solute arrival. Hence, it may be difficult to distinguish these processes. Furthermore, matrix diffusion and rate-limited sorption-desorption may also be indistinguishable under certain conditions. The effect of matrix diffusion decreases with increasing pumping rate, for shorter distance between the wells of the dipole, and for decreasing rate coefficients (i.e. smaller matrix porosity or smaller matrix sorption capacity and/or smaller diffusion coefficient and/or larger aperture). For the MDE a single injection well is considered, and the breakthrough is monitored at a control surface encircling the well. Matrix diffusion combined with possible equilibrium sorption in the matrix are the only mass transfer processes considered. Apart from the general objectives given above, a specific objective of the MDE is to investigate the effect of spatial variability in transmissivity on the diffusion process and the resulting diffusion-affected breakthrough. The diffusion rate parameter is correlated to the travel time through a joint probability density function. Both positive, negative and zero correlations are investigated. It was found that the effect of the

imposed correlation was moderate. Furthermore, if an effective value of the rate coefficient is to be used, the harmonic mean most closely resembles the case with zero correlated variable rate coefficient. The dependence of the calculated breakthroughs on pump rate, travel distance and rate coefficient is in the case of matrix diffusion presented in a dimensionless form for given transmissivity statistics and boundary conditions. The dimensionless diagrams provide a simple tool for scoping calculations when specific design constraints for the planned experiments are required. These nomograms could with minimal effort also be produced for other relevant transmissivity statistics and boundary conditions.

In summary the following specific design related recommendations and constraints are put forward for the MWTE experiment;

- A multitude of tracer "cocktails", which can be injected simultaneously in a given injection point, will be necessary. One of the tracers should be truly inert whereas the equilibrium surface sorption retardation factor of the sorbing species should not exceed 100 in order to produce practical time frames of the experiments. The selected tracers should also be mutually chemically inert, i.e. no chemical reactions between tracers.
- The use of different pumping rates, in combination with the use of tracers with different sorption characteristics, will facilitate in the discrimination between various rate-limited mass transfer processes.
- We do not consider it fruitful to put forward a specific fracture transmissivity or range of transmissivities since it is going to be difficult to find that particular fracture. Most probably other fracture properties will be more important; the singularity of the fracture, its continuity and the number of oblique fracture intersections in the fracture area of interest. When a fracture has been targeted and quantified, the resulting nomograms provide a tool for selecting optimal pumping rates and distances between boreholes.

With regard to the MDE the general recommendations above apply. Similarly to the MWTE, the nomogram produced for the MDE can be used for further scoping on desired breakthroughs when a specific fracture has been targeted. However, in order to suggest specific experimental conditions for the MDE we feel that further work and calculations are needed on how the diffusion front develops in the rock matrix.

BACKGROUND AND INTRODUCTION

In this chapter a short rationale and background to the performed scoping calculations for the detailed scale experiments are given in 1.1 and 1.2. In 1.3 the scope and objectives of the present study are given.

1.1

RATIONALE BEHIND DETAILED SCALE EXPERIMENTS

The near-field rock around the deposition holes plays two major roles with regard to repository performance; 1) it should provide a stable mechanical and chemical environment for the engineered barriers, 2) it should reduce and retard transport of any radionuclides released from the engineered barriers.

In the near-field it is conceptually envisaged that the existing fractures control transport of radionuclides. In order to realistically describe radionuclide transport in individual fractures there is a need to get an understanding of the flow velocity distribution in the fracture planes. In addition there is a need to understand the retardation mechanisms in the fractures. The latter include sorption and matrix diffusion effects.

One of the defined stage goals for the Operation Phase of the SKB Äspö Hard Rock Laboratory is to test models for groundwater flow and radionuclide migration /SKB, 1992/. Specifically, a project focused on the flow and transport processes in a detailed scale has been defined /Olsson, 1992/, focusing on;

- improved understanding of transport processes and refined conceptualization of radionuclide transport in single fractures,
- determination of in-situ parameters of the processes which control transport of sorbing radionuclides in single fractures,
- assessment of spatial variability in flow and transport parameters in fractures of different character.

Two detailed test plans for experiments on a detailed scale have been defined /Olsson, 1992/. The Multiple Well Tracer Experiment (MWTE) is planned to constitute a platform for assessment of validity and discrimination between different conceptual approaches/models

for transport in a single fracture. The Matrix Diffusion Experiment (MDE) is planned to demonstrate that matrix diffusion is a significant retardation mechanism for transport of reactive radionuclides over longer times.

The foreseen experimental set up of the MWTE is a multiple borehole array intersecting the fracture at different locations. The establishment of the optimal layout of this array is one of the objectives of the ongoing scoping calculations. The experimental concept behind the MWTE experiment is that important transport parameters can be evaluated from cross-hole tests in the same fracture, by applying different boundary conditions. The use of varying boundary conditions will allow inference of the importance of flow velocity on dispersion. In addition the use of a variety of tracers will facilitate evaluation of sorption and matrix diffusion phenomena. The posed idea to conduct a sequence of experiments where the parameters included in the transport models are varied systematically, and over a wide range, thereby provides a basis to distinguish between conceptual models, to assess the relative importance of processes under different conditions, and to determine effective transport parameters.

The rationale behind the MDE is the fact that due to practical constraints the tracer tests performed in the MWTE will be of limited time duration. Use of such short-time data for long-term predictions of sorption/matrix diffusion phenomena are therefore associated with uncertainty. Therefore, in the MDE, a sorbing tracer is planned to be injected into a single fracture at a low flow rate and for a period of several years. Subsequently the fracture will be excavated, and the fracture and the surrounding rock will be dissected and analysed for tracer. It is expected that significant amounts of tracer will remain close to the source, and that the concentration profile in the rock matrix will provide quantitative evidence of matrix diffusion.

1.2

DETAILED SCALE EXPERIMENTS IN PERSPECTIVE

An extension of the above project(s) is flow and transport experiments on a block scale. The objectives of these subsequent experiments are:

- to characterize and understand flow and transport in a minor fracture zone and its connection to the surrounding fracture network in three dimensions (30-50 m cube), and
- to obtain data on effective transport parameters at a block scale (50 m cube).

The results of this project will provide data which can be used to test

and refine models used to describe transport of radionuclides in fractured rock /Olsson, 1992/. This process will eventually provide guidance as to the choice of model approaches to be used in the description of near-field radionuclide transport in the licensing of a final repository for spent nuclear fuel. The conceptual understanding of flow and transport in individual fractures of the studied interconnected network of fractures relies profoundly on the results of the experiments on a detailed scale.

1.3

SCOPE OF WORK PERFORMED

The work presented in this report constitute scoping calculations to provide guidance for the experimental set-up, and testing philosophy of the two detailed scale experiments. This in order to ascertain experimental conditions under which the various mass transfer processes are possible to be observed and discriminated. The mass transfer processes can be separated into equilibrium and non-equilibrium (rate-limited) processes. An equilibrium process implies that the rate of mass transfer is high relative to the rate at which the tracer is being advected through the fracture. A non-equilibrium process implies that the rate of mass transfer, relative to the advection rate, is too low to assume the process as being instantaneous. In the present context *surface sorption* and *sorption in the rock matrix* are considered *equilibrium processes*; *diffusion into the rock matrix* and mass transfer resistances associated with *diffusion into stagnant water zones* are considered *rate-limited*.

The issues addressed specifically in the scoping calculations performed for the MWTE are;

- to study different non-equilibrium mass transfer processes on the transport of reactive tracer in a variable transmissivity fracture,
- to optimize experimental conditions in order to facilitate the identification and discrimination of the processes above,
- to formulate the conditions above in a very general format, e.g. using nomogram representation of the results of the scoping calculations.

The scoping calculations of the matrix diffusion experiment (MDE) address the following specific issues;

- the effect of matrix diffusion on the transport of a tracer injected in a well,
- optimization of experimental conditions to facilitate identification

of matrix diffusion,

- the effect of variability in the effective diffusion parameter in the model.

MATHEMATICAL DESCRIPTION

In this chapter the conceptual model and corresponding mathematical descriptions used are presented. In 2.1 a solution for diffusion into the rock matrix is presented and a solution technique for the coupling of rate-limited mass transfer reactions and conservative travel time distributions is discussed. In 2.2 a corresponding solution for surface sorption is presented. In 2.3 the flow and transport models which yield the travel time distribution is presented. Finally, in 2.4 a methodology for correlating the diffusion parameter with the travel time is discussed.

2.1 DIFFUSION MODEL

A streamline in a single fracture within a rock mass is considered. The fracture lies in the x - z plane and the aperture of the fracture is δ in the y direction, c.f. Figure 2-1. The streamline is not necessarily straight, it may be curved or meandering in the fracture plane; however, the length along the streamline, λ , is a single-valued function of x due to the prevailing hydraulic conditions. The velocity of a particle advecting along the streamline can then be defined as $w(\lambda)$. Even though the velocity is a function of λ only, the multidimensionality of the particle movement is retained due to the Lagrangian nature of w /Selroos and Cvetkovic, 1992/.

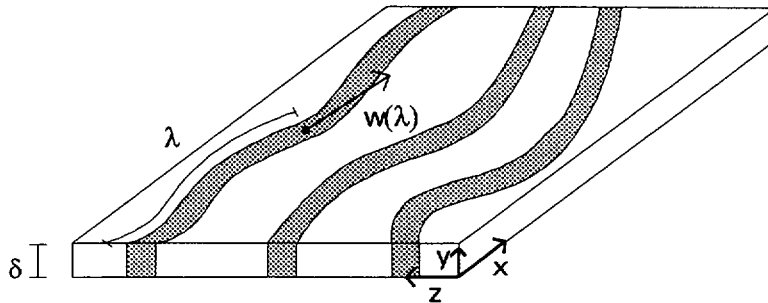


Figure 2-1. Fracture plane with aperture δ . The velocity at a distance λ along the first streamline is w .

The solute advecting along the streamline is subject to diffusion in the y direction; i.e. in the direction perpendicular to the fracture plane. If the solute flux, areally integrated over the y - z plane, is denoted by s_f in the fracture and by s_m in the matrix, mass balance equations for the fluxes may be written as /Cvetkovic, 1991/

$$\frac{\partial s_m}{\partial t} = D \frac{\partial^2 s_m}{\partial y^2} \quad (1)$$

$$\frac{\partial s_f}{\partial t} + w(\lambda) \frac{\partial s_f}{\partial x} = k \frac{\partial s_m}{\partial y}$$

In (1) D is the effective diffusion coefficient and $k = 2D\theta/\delta$, where θ is equal to the matrix porosity for a solute which does not sorb in the matrix and equal to a volume sorption coefficient multiplied by the rock bulk density, $K_d\rho$, for solutes which undergo equilibrium sorption in the matrix /Neretnieks, 1980/. Even though the true aperture may vary along the streamline an equivalent value is used in the calculation of the constant k . The other assumptions implicit in the derivation of (1) are as follows:

- no longitudinal dispersion
- diffusion only in the y direction
- well-mixed conditions over the cross-sectional area of the fracture
- no advection in the matrix
- a homogeneous and infinite rock matrix

For an instantaneous injection of one particle the solution of (1) in term of the flux s_f , normalized with the particle mass m , is /Tomasko, 1987; Cvetkovic, 1991/

$$\frac{s_f(t, \tau)}{m} = H(t - \tau) \frac{k^* \tau}{2\sqrt{\pi}(t - \tau)^{3/2}} \exp\left[\frac{-(k^* \tau)^2}{4(t - \tau)}\right] \quad (2)$$

where τ is the travel time of the solute particle along the streamline from the location of injection to the location where the flux is measured, $k^* \equiv k/\sqrt{D} = 2\theta\sqrt{D}/\delta$, and H is the Heaviside function defined by $H(t-\tau)=1$ for $t \geq \tau$ and $H(t-\tau)=0$ for $t < \tau$. The solution (2) is

thus expressed in terms of time t , travel time τ and the constants m and k^* only. It should be noted that the model (1) and solution (2) only describe diffusion into the rock matrix with possible equilibrium sorption in the matrix. Surface sorption is not included in the model. However, surface sorption is easily included by multiplying the first term in the second equation in (1) with a surface sorption retardation factor, R . In the solution (2) τ is then replaced by τ/R , and in the calculation of k the diffusion coefficient D is replaced by D/R .

Due to aperture variability and imposed hydraulic boundary conditions a set of discrete streamlines may be formed within the fracture plane. These streamlines may have varying velocities and show a non-uniform pattern, rather than a parallel one, due to the physical and hydraulic conditions. When several particles of a total mass M are injected instantaneously into the fracture plane at $x=z=0$ different particles will advect along different streamlines; the expected mass flux at position $x=L$ measured over a control plane (CP) perpendicular to the x direction is

$$\bar{s}_f(t; L) = M \int_0^{\infty} s_f(t, \tau) p_{\tau}(\tau; L) d\tau \quad (3)$$

where p_{τ} is the probability density function (pdf) of travel time expressing the probability of arrival at L as a function of time. Depending on the physical properties of the fracture and the imposed hydraulic conditions various pdfs will arise. In section 2.3 it will be discussed how these pdfs can be obtained.

2.2

SORPTION MODEL

The methodology of separating rate-limited mass transfer and transport under heterogeneous flow conditions into separate solutions with subsequent integration, as outlined in section 2.1 for matrix diffusion, may be used for other mass transfer reactions as well.

If a non-equilibrium sorption-desorption reaction controlled by first-order kinetics is present the solution for the mass flux in the fracture is /Lassey, 1988; Cvetkovic and Shapiro, 1990/

$$\frac{s_f(t, \tau)}{m} = \exp(-k_1 t) \delta(t - \tau) + k_1 k_2 \tau \exp(-k_1 \tau - k_2 t + k_2 \tau) \hat{I}_1[k_1 k_2 \tau(t - \tau)] \quad (4)$$

where δ is the Dirac delta function, $\hat{I}_1(z) = I_1(2\sqrt{z})/\sqrt{z}$, I_1 is a modified Bessel function of the first kind of order one, and k_1 and k_2 are forward and reverse rate coefficients, respectively. The expected solute flux is subsequently obtained using the solution (4) in the integration in (3).

The kinetic model (4) can be used to describe rate-limited mass transfer of both chemical and physical origin /Weber et al., 1991/. In the present context mass transfer associated with diffusion into stagnant water zones, or zones with very low hydraulic conductivity, is considered. A limitation in the model (4) is that the sorption parameters k_1 and k_2 are not expressed in terms of other system parameters such as k is in the diffusion model (1). However, the general features of rate-limited processes may be studied through the utilization of this model.

2.3 FLOW AND NONREACTIVE TRANSPORT MODELS

In this section the flow and transport models used will be introduced. The result, or output, from these models is the travel time distribution which is needed for the calculations in 2.1 and 2.2. Through the flow model streamlines are obtained; subsequently the transport model yields the breakthrough using a particle tracking methodology. Depending on the physical characterization of the fracture (homogeneous/ heterogeneous aperture properties) different flow models are utilized.

2.3.1 Homogeneous flow

When the aperture of the fracture is assumed constant, analytical solutions are available for the resulting equipotential lines and streamlines given the prevailing hydraulic conditions. In this study multiple (two-well) and single well configurations are considered.

2.3.1.1 **Single well configuration**

Consider an infinite fracture plane with a constant aperture δ . A borehole fully penetrating the fracture injects water with a flow rate Q . Circular equipotential lines with straight streamlines are formed. If the hydraulic conductivity of the fracture is K , i.e. the transmissivity is $T=K\delta$, the hydraulic head along a streamline can be calculated as

$$h(x) = \frac{Q}{2\pi T} \ln(x) + C \quad (5)$$

where x is the distance along the streamline from the injection point to the monitoring point and C is a constant equal to the known head value at some given distance. Using (5) the head distribution may be obtained analytically along the streamlines.

2.3.1.2 **Dipole well configuration**

Consider two boreholes in the same infinite and homogeneous fracture as discussed above in 2.3.1.1. The boreholes are located at $(\pm a, 0)$. In one borehole water is injected with a flowrate Q , in the other borehole water is abstracted with the same flowrate. If we denote by r_1 and r_2 the radii drawn to any point in the x - z plane from the points $(\pm a, 0)$, and by θ_1 and θ_2 the angles which these radii make with the positive direction of the x axis, then the head h and streamlines Ψ in the fracture plane are given by /Lamb, 1945/

$$\begin{aligned} h &= -\mu \log(r_1 / r_2) \\ \Psi &= -\mu(\theta_1 - \theta_2) \end{aligned} \quad (6)$$

where $\mu = Q / (2\pi T)$ and the different streamlines are obtained for different values of the constant $C = \theta_1 - \theta_2$. In short, circular streamlines can be constructed using the second relation in (6), by identifying the radii r_1 and r_2 on the streamlines and using the first relation in (6) the head distribution in the fracture plane can be obtained.

2.3.2 **Heterogeneous flow**

For cases where the aperture δ is spatially variable analytical solutions for the streamlines and head distribution are generally not available. Alternatively numerical simulations may be performed. In the present study a stochastic continuum Monte Carlo approach is used.

The transmissivity of the fracture plane is considered a random space variable (RSV) which is log-normally distributed and characterized by an exponential spacial correlation structure. Synthetic transmissivity fields are generated using the Turning Bands (TUBA) method /Mantoglou, 1987/. The transmissivity values are transformed into

hydraulic conductivity values using an equivalent aperture value constant over the domain. In each conductivity field the 2D flow equation is solved with given boundary and pumping conditions and assuming steady-state flow conditions. A block-centered finite difference scheme employing direct band elimination is used in the numerical solution for the head distribution.

2.3.3 **Nonreactive transport**

After the head distribution is obtained for the homogeneous or heterogeneous flow fields the velocity distribution is calculated in discrete points using Darcy's law. Solute transport is subsequently modelled using a numerical particle tracking scheme which incorporates non-reactive advection only. Local dispersion and molecular diffusion are consequently neglected; the spread of the particles is due to the variable velocity field only. The assumption of no dispersion along the streamline is in parity with the assumptions used for the diffusion model in 2.1 and the sorption model in 2.2.

The travel time of each individual particle from its point of injection along the streamline to the location of measurement λ is obtained as

$$\tau(\lambda) = \int_0^{\lambda} \frac{d\lambda'}{w(\lambda')} \quad (7)$$

where w is the Lagrangian velocity along the streamline introduced in 2.1. In each realization a solute breakthrough is obtained which reflects the prevailing pumping conditions. For homogeneous cases this breakthrough is the travel time pdf needed for evaluating the diffusion affected mass flux in (3); for heterogeneous cases an averaging over all breakthroughs resulting from the individual realizations yields the travel time pdf. The pdf obtained thus reflects both the pumping conditions and the heterogeneous transmissivity field.

2.4 **DIFFUSION CORRELATED WITH TRAVEL TIME**

In the previous sections a methodology has been presented on how to obtain the diffusion-affected breakthrough using a conservative travel time pdf and the solution for diffusion in (2). It is emphasized that an equivalent aperture value is assumed along the streamline in the calculation of k^* in (2); furthermore, the same equivalent aperture value is used for all individual streamlines when the integration is

carried out in (3). However, for some flow conditions a correlation may exist between the travel time and the aperture. Hence, if this correlation is to be reflected in the calculation of the expected flux, then equation (3) should be replaced with

$$\bar{s}_f(t) = \int_0^{\infty} \int_0^{\infty} s_f(t, \tau, k^*) p_{\tau, k^*}(\tau, k^*) d\tau dk^* \quad (8)$$

where p_{τ, k^*} is the joint pdf for τ and k^* , and s_f is a function not only of time and travel time but also of the equivalent k^* value along each streamline.

In order to evaluate (8) the joint pdf p_{τ, k^*} is needed. The numerical simulations discussed above only yield the pdf of travel time. Hence a joint pdf distribution has to be assumed for the correlated case. However, the travel time moments for this distribution may be estimated from the numerical simulations. The assumption of a log-normal distribution yields the following expression for the joint pdf

$$p_{\tau, k^*}(\tau, k^*) = \frac{1}{2\pi\tau k^* \sigma_{\ln\tau} \sigma_{\ln k^*} \sqrt{1-\rho^2}} \exp \left[-\frac{1}{2(1-\rho^2)} \left(\frac{(\ln \tau - \mu_{\ln\tau})^2}{\sigma_{\ln\tau}^2} - \frac{2\rho}{\sigma_{\ln\tau} \sigma_{\ln k^*}} (\ln \tau - \mu_{\ln\tau})(\ln k^* - \mu_{\ln k^*}) + \frac{(\ln k^* - \mu_{\ln k^*})^2}{\sigma_{\ln k^*}^2} \right) \right] \quad (9)$$

where ρ is the coefficient of correlation between T and k^* , μ and σ^2 are the mean and variance of the parameters indicated by their respective subscripts. It is finally noted that incorporation of correlation through (9) is meaningful only when the travel time distribution in some manner reflects the aperture distribution. If the travel time distribution is a function only of the prevailing pumping

conditions and not of the aperture distribution, then the use of (9) will introduce a false correlation.

FRACTURE PROPERTY DATA

In this chapter an overview is given on relevant fracture property data. In 3.1 different equivalent aperture values and their relationship to conductivity and transmissivity values are addressed. In 3.2 the spatial variability of fracture properties is discussed; finally, in 3.3 the generic data used for the present study is presented.

3.1 TRANSMISSIVITY AND APERTURE MEASUREMENTS

Few (if any) directly measured fracture transmissivities have been reported in the literature. In most cases the published fracture hydraulic properties are presented as equivalent fracture apertures calculated from tracer tests. We distinguish between two types of "tracer apertures", the mass balance aperture δ_m , the frictional loss aperture δ_f , and a "hydraulic aperture", the cubic law aperture δ_c . Confusion has existed with regard to reported "equivalent apertures" where the different concepts sometimes have been misrepresented. Tsang /1992/ has sorted out the theoretical background behind the different definitions introduced by Abelin et al. /1985/, and has also sorted out differences reported in the literature.

For a realistic fracture where apertures constitute a heterogeneous random field in two dimensions, it can be shown that the three defined equivalent apertures may be ranked as $\delta_m > \delta_c > \delta_f$. From the single fracture experiment at Stripa /Abelin et al., 1985/, the interrelationship above holds for both linear and radial flow assumptions. The frictional loss aperture δ_f was found to be on the order of 1 μm , and the ratio $\delta_m:\delta_c:\delta_f$ is approximately 1000:10:1 /Abelin, 1985/. Pressure pulse testing in the same fracture evaluated assuming radial flow conditions and inferences based on natural flow in the fracture towards the drift yielded transmissivities ranging between 1×10^{-10} and 8×10^{-10} m^2/s . Similar values are also reported from characterization of the holes used for injection of tracer during the so-called channelling experiment /Abelin et al., 1990/.

Other sources for fracture transmissivity are fracture transmissivity distributions inferred indirectly from distributions of packer test transmissivity data. The inference is based on probabilistic models

which includes the frequency of conductive fractures, $p_c \lambda_f$, and a model defining the fracture transmissivity distribution which could be either a Gamma distribution /Osnes et al., 1991/ or a log-normal distribution /Derschowitz et al., 1991/. These type of models have been applied on the site characterization data collected as part of the KBS-3 study /Osnes et al., 1991/ and on the Finnsjön and Äspö data sets as a part of discrete fracture network modelling exercises /Axelsson et al., 1989; Geier et al., 1992/.

3.2

SPATIAL VARIABILITY OF HYDRAULIC PROPERTIES

Aperture measurements have been reported in the literature to enable inference of fracture roughness characteristics, e.g. Swan /1985/. The hydraulic aspects of aperture variation have been studied using different laboratory techniques with varying success; plastic film pressed in between the fracture surfaces /Iwai, 1976/, measurements of heights of asperities on both sides and subsequent inference of aperture by subtraction, injection of Woods metal and subsequent mapping of points of contact and the aperture variation of voids /Pyrak-Nolte et al., 1987/, resin injection and subsequent measurements on cut slices of rock/resin. Hakami /1989/ made plastic replicas of the fractures for inference of fracture apertures. All studies above have been made on large diameter cores or natural excavated fracture surfaces of minor size. There are few accounts of spatial variability of aperture over the exposed fracture area. Abelin et al. /1990/ reports variograms of visual apertures with correlation lengths of 0.05 to 0.20 m from field studies in the Stripa mine. Kriging was subsequently used to estimate the fracture aperture distribution over the fracture plane. Similarly the flow variability was used to generate a transmissivity distribution.

Tsang and Tsang /1987/ used a stochastic variable aperture model to model channelized flow in individual fractures. The spatial variability of fracture aperture is here described as the ratio λ/L between correlation length λ of the aperture to the channel length L , allowed to vary between 0.05 and 0.2. In subsequent analysis a ratio of 0.1 between correlation length (of aperture) and unit domain size is used /Moreno et al., 1988; Tsang and Tsang, 1989; Moreno et al., 1990/. This relationship is also used by Nordqvist et al. /1992/ when assigning heterogeneous fracture aperture variation within individual fractures of a discrete fracture network.

A mathematical relationship between the cubic law aperture δ_c and the frictional loss aperture δ_f with the natural log (ln)-aperture variance σ_p^2 as the sole parameter has been presented by Brown /1984/

$$\delta_l = \delta_c \left[(1 - \sigma_\beta^2) \left(1 - \frac{\sigma_\beta^2}{2(1 - \sigma_\beta^2)^2} \right) \right]^{1/2} \quad (10)$$

Gustafsson and Klockars /1981/ found that δ_c is approximately a factor 20 larger than δ_l . Brown /1984/ used this relationship together with equation (10) to calculate a ln-aperture variance $\sigma_\beta^2 \cong 0.5$. Also using the data provided by Gustafsson and Klockars /1981/ Brown /1984/ calculated the correlation length λ of the aperture to be 0.2 m using

$$D_{11} = 4u\lambda\sigma_\beta^2 \exp(2\sigma_\beta^2) \quad (11)$$

where D_{11} is dispersivity and u is the fluid velocity. The correlation length obtained is in accordance with values of λ reported by Abelin et al. /1990/.

3.3

FRACTURE PARAMETERS PERTINENT TO ÄSPÖ

The descriptive geological model of Äspö presented by Wickberg et al. /1991/ indicates that the geology at approximate 400 m depth, corresponding to the planned experimental depth, is heterogeneous although dominated by granodiorite-diorite with minor lenses of Småland granite and fine-grained granite. This means that a fracture likely to be found at this depth will be featured by fracture transmissivity characteristics derived from these rock types. Fracture transmissivity data have been inferred indirectly by statistical analysis of packer test data in fine-grained granite and Småland granite /Axelsson et al., 1989/ and in diorite /Liedholm, 1990/, c.f. Table 3.1.

Table 3-1. Representative statistical data of fracture transmissivity distributions derived from statistical analysis of packer test data and fracture logs from Äspö. Mean and standard deviations are given as \log_{10} -values.

Rock type	mean of $\log(T)$ T [m^2/s]	σ of $\log(T)$ T [m^2/s]	Source of information
Småland granite	-5.9	0.9	Axelsson et al. /1989/
Fine-grained granite	-7.3	1.4	Axelsson et al. /1989/
Diorite	-7.3	1.07	Liedholm /1990/

A mean \log_{10} -transmissivity $\log(T) = -7.3$ ($T = 5 \times 10^{-8}$ m²/s) has been selected as a representative value for a typical fracture at laboratory depth at the Äspö Hard Rock Laboratory. Our selected transmissivity is based on injection test data and subsequent statistical analysis. An aperture back-calculated from this transmissivity ($\delta_c = 41 \mu\text{m}$) should thus be regarded as a cubic law aperture. For our analysis of transport in an individual fracture we are, however, interested in the transport-related frictional loss aperture δ_f . Andersson and Klockars /1985/ in their analysis of a multiple borehole tracer test at Stripa found that the hydraulic conductivity of a fracture based on the cubic law is 40-50 times larger than that based on frictional losses, and depending on whether linear or radial flow symmetry is assumed. Using an assumption of radial flow this relationship gives us a mean "tracer aperture" of 5.8 μm . Using the cubic law

$$T_f = \frac{\delta_f^3 g}{12\nu} \quad (12)$$

where T_f = "tracer" transmissivity based on frictional loss [L]²/[T]
 δ_f = "tracer" aperture based on frictional loss [L]
 ν = kinematic viscosity ($\cong 1.124 \times 10^{-6}$ m²/s)
 g = acceleration due to gravity

based on this latter aperture gives us a mean (tracer) transmissivity $T_f = 1.42 \cdot 10^{-10}$ m²/s ($\log T_f = -9.85$). We do not have any site specific data from Äspö on the variance of the aperture within a fracture plane, but data from Stripa /Gustafsson and Klockars, 1981/ indicate a \log_{10} -value on the order of 0.09 /Brown, 1984/. Using elementary statistics applied to the cubic law relationship (12) we can estimate the variance of the \log_{10} -transmissivity T_f within an individual fracture to be $\sigma_T^2 = \text{var}(\log T_f) \cong 0.85$. In our analysis we use $\sigma_T^2 = 1.0$. Similarly, we do not have any site-specific data on the correlation length of transmissivity in an individual fracture plane, nor of the aperture in an individual fracture plane. For our analysis we select a correlation length of transmissivity in an individual fracture plane $\lambda_T = 1.0$ m. It should be noted that for aperture the corresponding measure appear to be on the order of a few decimeters, see above. The fracture hydraulic characteristics used in the subsequent scoping calculations are indicated in Table 3-2.

Table 3-2. Fracture hydraulic parameters used in the scoping calculations of the planned MWT and MD Experiments at Äspö

Parameter	Value	Source of information
T_l	$1.4 \times 10^{-10} \text{ m}^2/\text{s}$	inferred
σ_T^2	1.0	inferred
λ_T	1.0 m	inferred

MULTIPLE WELL TRACER EXPERIMENT

In this chapter scoping calculations for the Multiple Well Tracer Experiment (MWTE) are presented. In 4.1 the experimental setup of the MWTE is discussed; in 4.2 the results of the calculations are presented and discussed. Finally, in 4.3 some conclusions based on the obtained results are given.

4.1 EXPERIMENTAL SETUP

For the scoping calculations of the MWTE a design with two boreholes, one injection borehole and one abstraction borehole, is considered (Figure 4-1). The pumping rates are the same for both boreholes. A given mass of solute is injected instantaneously into the injection borehole. This simple configuration is motivated by the fact that it will yield the information requested on the interaction between rate-limited mass transfer and flow induced by pumping. An understanding of the combined processes under this simple flow configuration has to be obtained before the effect of more complex flow configurations are to be considered.

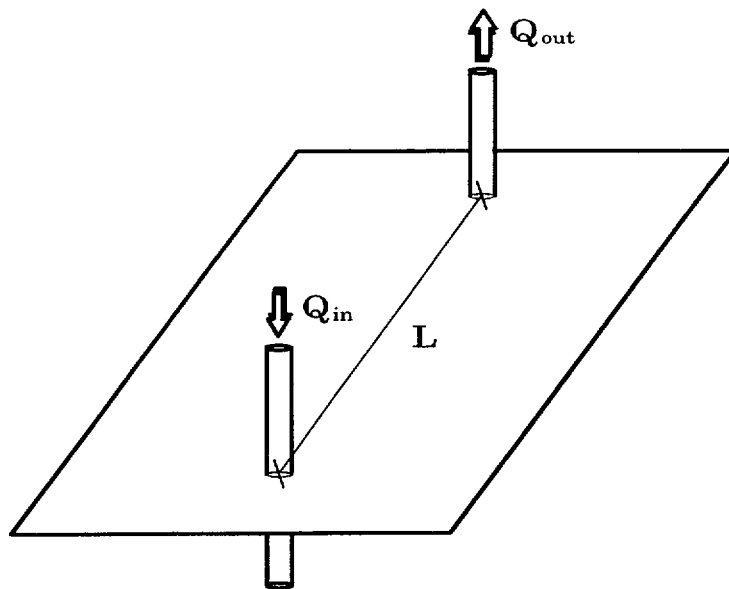


Figure 4-1. Experimental set-up for the MWTE with two boreholes separated by a distance L injecting and abstracting water at a flow rate Q .

4.2 DISCUSSION AND RESULTS

4.2.1 Matrix diffusion

When matrix diffusion is analyzed the solution presented in 2.1 is used. Depending on the flow conditions the flow model in 2.3.1 or in 2.3.2 is used.

4.2.1.1 **Homogeneous flow**

For a fracture plane with a constant aperture (and thus constant transmissivity) the dipole solution (5) can be used for obtaining the streamlines. Each streamline constitutes part of the circumference of a circle with a given radius. Different streamlines are thus defined by circles with different radii. The resulting solute breakthrough measured in the abstraction borehole will consequently be dispersed due to the varying lengths and velocities on the streamlines.

In Figure 4-2 the accumulated mass arrival for a conservative tracer is shown for a pumping case of $Q=5$ ml/h.

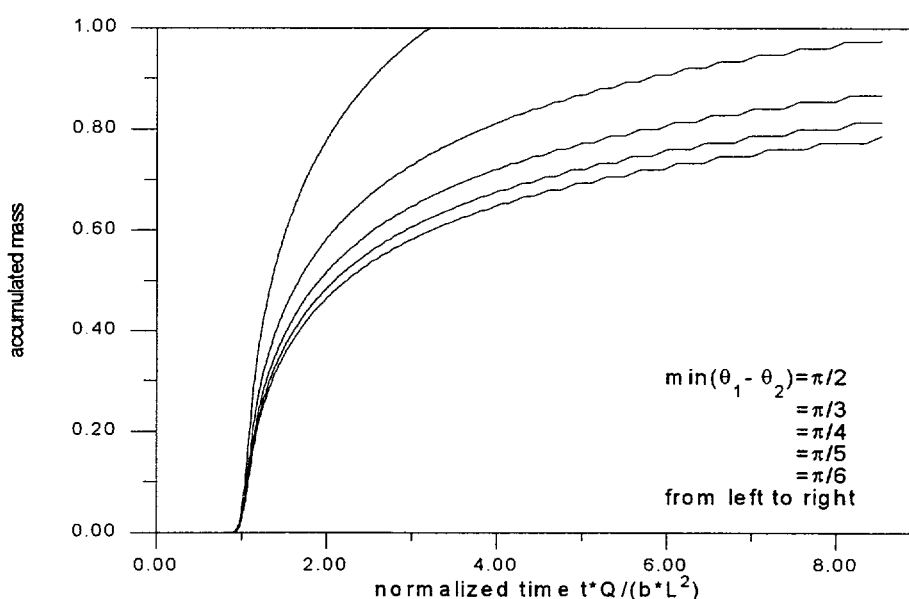


Figure 4-2. *Effect of streamline configuration on the cumulative breakthrough of mass in the abstraction borehole.*

The different curves correspond, from left to right, to cases with an increasing number of outer, slower, streamlines included. For the case with the minimum value of $(\theta_1 - \theta_2) = \pi/2$ the angle between the velocity vector associated with the outermost streamline and the

straight line between the two boreholes is 90° at the injection point. The flow field consequently covers 180° of the fracture plane surrounding the injection bore hole. Streamlines with initial velocity vectors having negative x components are thus excluded from the perfect dipole flow field. For the case with $(\theta_1 - \theta_2) = \pi/6$ the corresponding angle is 150° and the flow field covers 300° of the fracture plane around the injection bore hole; only streamlines in the remaining 60° sector are excluded from the perfect dipole in the calculations. The accumulated mass is normalized with the total mass advecting on the selected streamlines for each case. The total accumulated mass is thus equal to one for all cases. It can be observed that strong tailing results when a large number of outer streamlines are included in the calculation. However, for field scale tracer experiments a complete mass recovery from the slowest streamlines cannot be anticipated due to time constraints and practical limitations. Hence, when analyzing possible tailing from mass transfer reactions we choose in the following the flow case above with the least spreading. In the transport calculations 75 streamlines inside the 180° field are used to obtain the velocity field.

Matrix diffusion is added to the far left conservative breakthrough of Figure 4-2 using equations (2) and (3). The conservative breakthrough is interpreted as the travel time pdf. In Figure 4-3 the effect of various diffusion cases are shown together with the conservative case. The case with $k^* = 0.1 \text{ h}^{-1/2}$ corresponds to an assumed aperture of $\delta = 5.8 \text{ } \mu\text{m}$ (see section 3.3) together with a matrix porosity of $\theta = 0.001$ and a diffusion coefficient of $D = 2.5 \times 10^{-11} \text{ m}^2/\text{s}$.

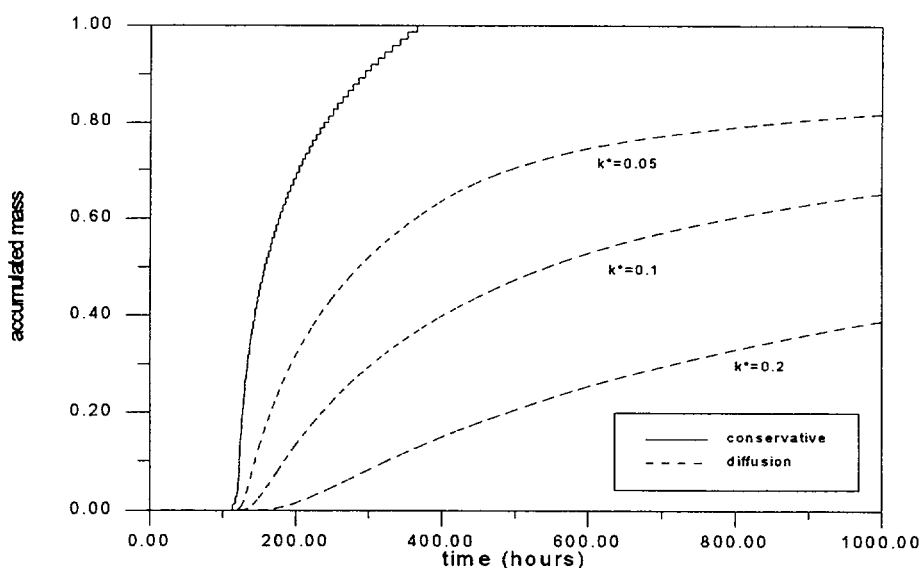


Figure 4-3. Influence of the magnitude of the k^* -value on the cumulative breakthrough.

The general effect of matrix diffusion is a delay in mass arrival. It can also be seen in Figure 4-3 that the solution is fairly sensitive to changes in the diffusion parameter k^* . Multiplying or dividing k^* by a factor two has apparent effects on the breakthrough. For diminishing values of k^* the solution converges to the nonreactive case, whereas for increasing values the mass flux approaches zero. Increasing k^* -values imply an increase in the effective diffusion parameter, an increase in the matrix porosity or in the matrix sorption capacity, or a decrease in the aperture.

The effect of pumping rate on the accumulated mass flux is showed in Figure 4-4 for the case of diffusion with $k^*=0.1$. For increased pumping rates, and shorter travel times, matrix diffusion is not developed to the same extent during the early breakthrough. This is due to the shorter contact times between the solute and the surrounding rock matrix. Correspondingly, for lower pumping rates the effect of matrix diffusion is more pronounced already during the early stages of the breakthrough.

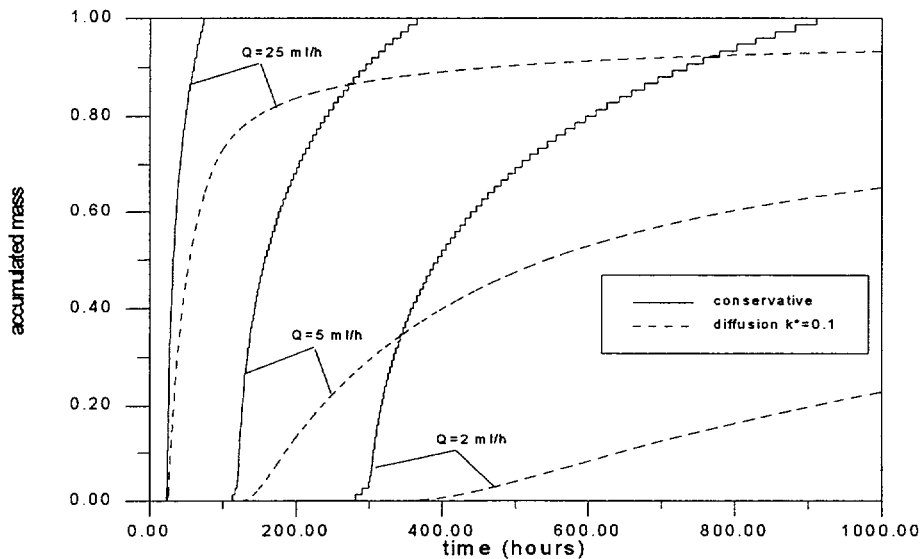


Figure 4-4. Effect of pumping rate on the cumulative breakthrough.

4.2.1.2

Heterogeneous flow

For cases where the aperture, and hence also transmissivity, is spatially variable the solution technique outlined in section 2.3.2 is used. In the Monte Carlo simulations 25 realizations are used to obtain the travel time pdf. The variance of the \log_{10} -transmissivity field is assumed to be equal to one; the correlation structure is assumed exponential with an integral scale equal to one meter (see section 3.3).

The injection of the solute mass in the numerical borehole is arranged in such a manner that the solute advects along a selected number of inner streamlines which correspond to the same selection of streamlines as in the homogeneous case. Hence the homogeneous and heterogeneous cases can be compared quantitatively.

In Figure 4-5 a comparison is made between the accumulated mass flux resulting from the homogeneous and heterogeneous flow conditions, respectively. Both conservative and diffusion affected ($k^*=0.1$) breakthroughs are shown. It can clearly be observed that the effect of heterogeneity is an increased spreading of the breakthrough with pronounced tailing. Furthermore, heterogeneity also results in some mass arrival prior to the first homogeneous mass arrival. When diffusion is included the differences between the homogeneous and heterogeneous breakthroughs are somewhat reduced; however, the heterogeneous case is still more spread with both more pronounced tailing and early mass arrival.

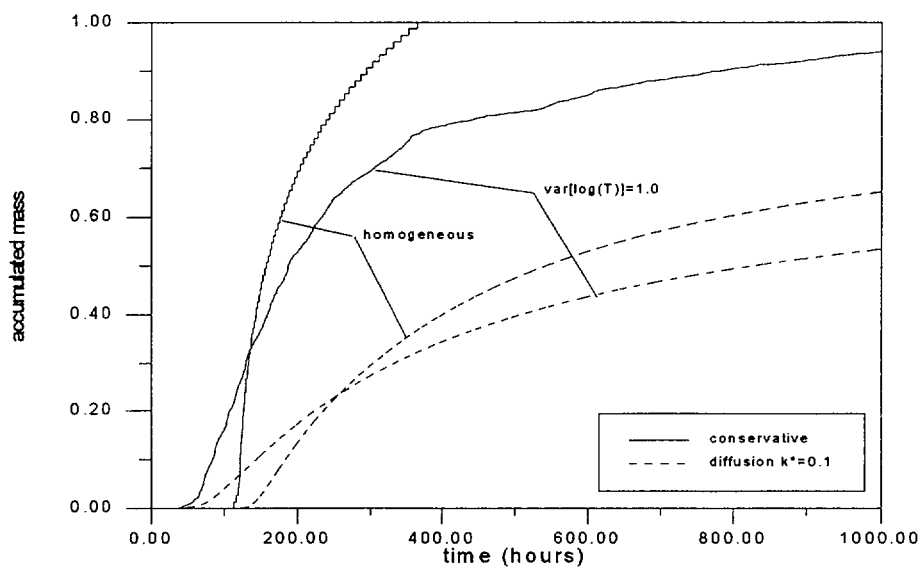


Figure 4-5. Comparison between conservative and diffusion affected cumulative breakthroughs for homogeneous and heterogeneous flow conditions.

When the solution to the diffusion equation (2) is applied to heterogeneous flow conditions with a spatially variable aperture it is somewhat unclear what equivalent aperture δ should be used in the calculation of the diffusion parameter k^* . In Figure 4-5 the k^* value is based on the frictional loss (tracer) aperture δ_i ; however, if we use the cubic law aperture, which is an order of magnitude larger than the tracer aperture, k^* will be an order of magnitude smaller. The effect of such a reduction in k^* is shown in Figure 4-6; it can be seen that

the effect of matrix diffusion practically disappears for the conditions selected when the cubic law aperture is used. The effect of a tenfold increase in k^* is also shown in Figure 4-6. However, this scenario is unlikely due to the fact the frictional loss aperture is the smallest equivalent aperture (see section 3.1)

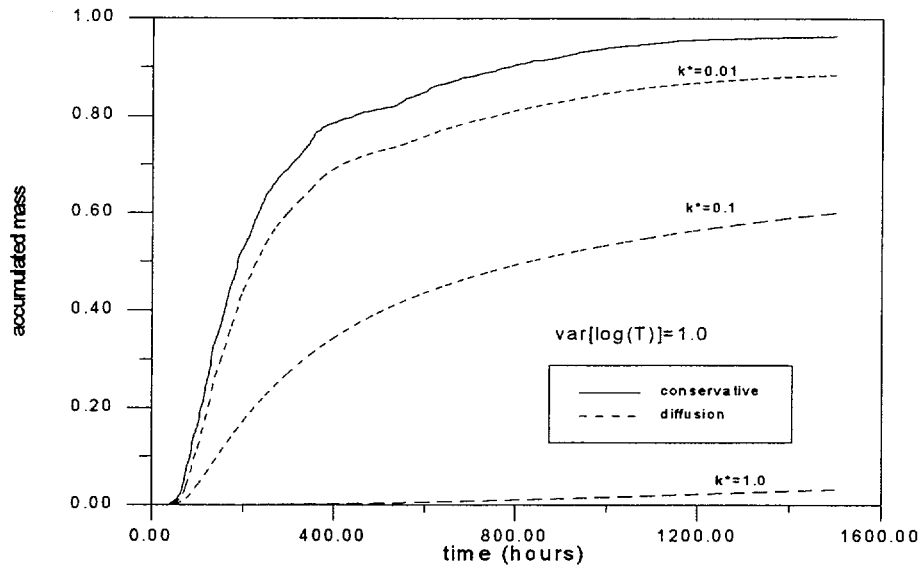


Figure 4-6. Effect of a tenfold increase or decrease in the diffusion parameter k^* on the cumulative breakthrough.

The effects of different pumping rates, together with the effects of different diffusion parameters k^* , may be expressed in a non-dimensional form. This is shown in the nomogram in Figure 4-7; a normalized time, $tQ/(\pi\delta L^2)$, and a normalized diffusion parameter, $k^*/[Q/(\delta L^2)]^{1/2}$, are introduced. The information in the nomogram thus pertains to any combination of pumping rates Q , distances between boreholes L , equivalent apertures δ , and diffusion parameters k^* . However, the nomogram is specific for the variability, boundary and initial (injection) conditions chosen. A similar nomogram as in Figure 4-7 could also be produced for the homogeneous case discussed in section 4.2.1.1.

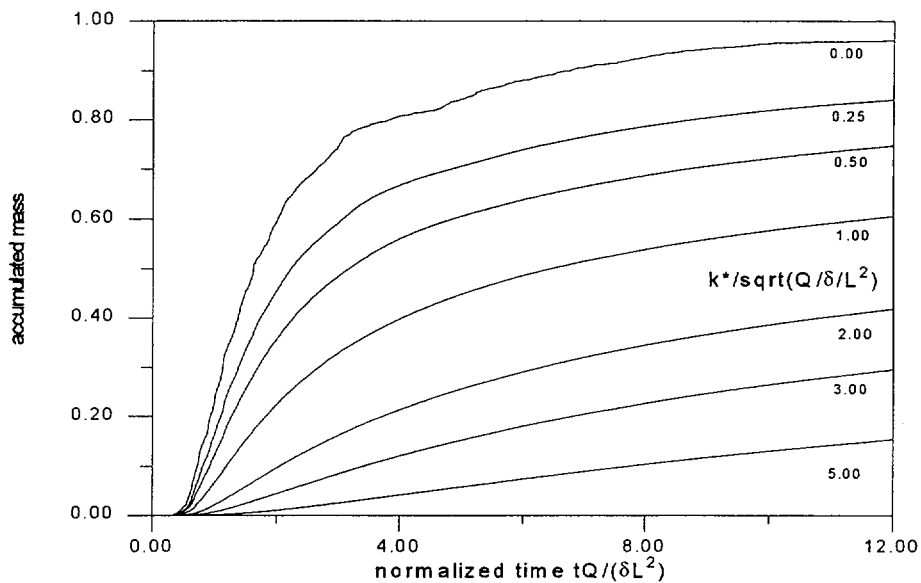


Figure 4-7. Dimensionless nomogram presentation of the results for the given transmissivity statistics.

4.2.2

Rate-limited surface sorption

Non-equilibrium sorption models are frequently used to describe mass transfer processes such as diffusion into stagnant, or immobile, water zones. Non-equilibrium sorption is thus similar to matrix diffusion in the sense that it is a rate-limited process. Consequently the mass flux of a solute subject to non-equilibrium sorption may be expected to show some features similar to a breakthrough affected by matrix diffusion.

In Figure 4-8 the accumulated mass flux using equation (4) in the integration in (3) is shown for different sorption cases. The hydraulic conditions correspond to the homogeneous case of Figure 4-3. For the cases presented in Figure 4-8 the forward and reverse rate sorption coefficients (k_1 and k_2) are assumed equal; the arrow in the figure indicates the evolution of the solution for increasing values of the equal sorption coefficients. The solution shows slightly different features than the matrix diffusion solution; specifically, for sorption coefficients approaching infinity the solution converges to the equilibrium sorption case with a retardation factor defined as $R = 1 + k_1 / k_2$ (breakthrough curve most to the right in Figure 4-8). The diffusion affected breakthrough converges to zero for diffusion parameters approaching infinity (Figures 4-3, 4-6 and 4-7). However, for intermediate non-equilibrium sorption cases breakthroughs may be identified which fairly closely resemble diffusion-affected breakthroughs (Figures 4-3 and 4-8). This is particularly true for diffusion combined with high pumping rates (Figures 4-4 and 4-8).

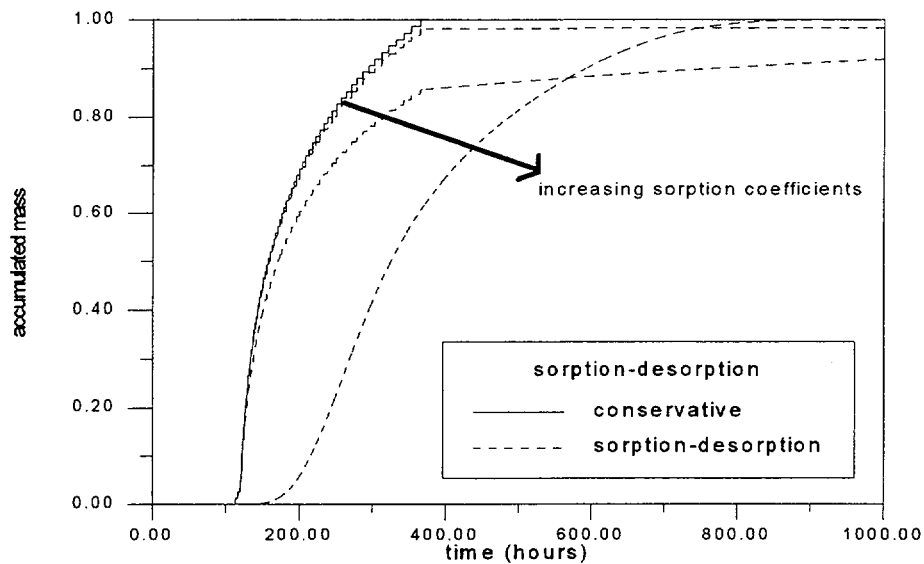


Figure 4-8. Effect of increasing sorption coefficients on the cumulative breakthrough.

4.3

CONCLUSIONS

Tailing and delay in breakthrough may result from a number of different processes/phenomena. These include e.g. heterogeneity in transmissivity, flow induced by dipole pumping, and rate-limited mass transfer reactions such as matrix diffusion or diffusion into stagnant zones which can be described as non-equilibrium sorption.

Consequently it may be impossible to identify the active processes by analyzing one breakthrough only. However, the effect of mass transfer may be characterized either by using different pumping rates (Figure 4-4), and/or by comparing conservative and reactive tracers. The tailing resulting from a conservative tracer test, or from a tracer test where rate-limited processes are negligible due to the short contact times, may be attributed to the prevailing heterogeneity and pumping conditions. It should in this context also be emphasized that when a rate-limited mass transfer reaction is present it may not be an easy task to determine whether the active process is matrix diffusion, diffusion into stagnant zones, or a combination of both processes.

The assignment of values to the rate parameters of the models used is an open question. For the matrix diffusion solution (2) the equivalent aperture is not well defined for heterogeneous cases (Figure 4-6). For the non-equilibrium sorption solution (4) the rate coefficients are at present not related to other measurable system parameters. These limitations have to be overcome before the models may serve for real-case transport predictions and safety assessment studies.

It should be emphasized that the results presented in this chapter are dependent on the choice of included streamlines, c.f. Figure 4-2.

However, the presented methodology is generic; wider flow fields can easily be included in actual design calculations if so preferred. Furthermore, in the numerical simulations dipole flow fields of unequal strength may also readily be adopted. Finally, if the presented methodology is to be used for analysis of conducted tracer tests rather than for design calculations of such experiments, it is important to calibrate the number of streamlines in the numerical model such that observed and modelled conservative breakthroughs match. Such an exercise is, however, beyond the scope of this report.

MATRIX DIFFUSION EXPERIMENT

In this chapter scoping calculations for the Matrix Diffusion Experiment (MDE) are presented. In 5.1 the experimental setup of the MDE is discussed; in 5.2 the results of the calculations are presented and discussed. Finally, in 5.3 some conclusions based on the obtained results are given.

5.1

EXPERIMENTAL SETUP

For the scoping calculations of the MDE a design with one borehole only is considered (Figure 5-1). The hydraulic properties of the rock are assumed to be the same as those for the MWTE (sections 3.3 and 4.1). A given mass of solute is injected instantaneously into the borehole, and the breakthrough of mass is monitored at a control surface encircling the injection borehole (indicated in Figure 5-1). For a fracture with homogeneous hydraulic properties the monitored mass flux will be a pulse. The radial distance between the borehole and the monitoring surface, L , is assumed to be on the order of a few meters; the injection rates, Q , are assumed to be lower than those for the MWTE.

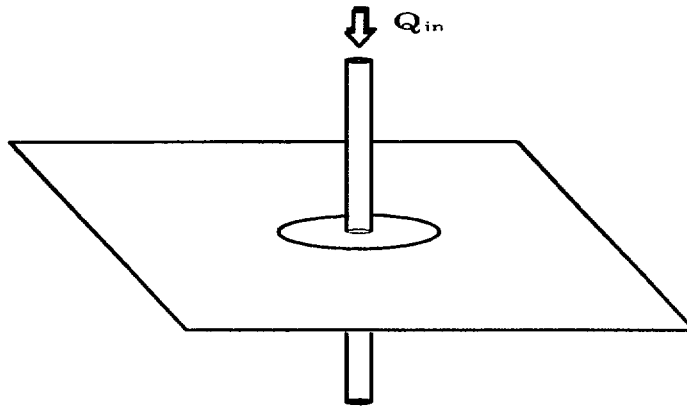


Figure 5-1. Experimental set-up for the MDE with one centrally located injection borehole. The control surface is indicated around the borehole.

DISCUSSION AND RESULTS

The methodology used for the MDE is the same as the one used for the MWTE in section 4.2.1. Furthermore, the conditions are the same except for the imposed pumping conditions. Consequently the results are expected to be similar; moreover, it should be possible to express the MDE results in a similar nomogram form as the MWTE results.

In Figure 5-2 dimensionless results are shown for conservative and diffusion affected breakthroughs for both the homogeneous and heterogeneous cases. It can be seen that the mass flux indeed is a pulse for the conservative, homogeneous case. When heterogeneity is included the breakthrough becomes more spread with pronounced early and late arrival. The effect of matrix diffusion is a strong spreading of the mass flux. As a matter of fact, when matrix diffusion is present the apparent spreading effect of heterogeneity is diminished during the tailing phase. In Figure 5-2 only one dimensionless diffusion case is shown for each heterogeneity case; however, nomograms similar to Figure 4-7 could be produced for each heterogeneity case. It should be noted that these nomograms would be specific for the heterogeneity case and initial conditions chosen. The information in the nomogram would pertain to any combination of pumping rates Q , radial distances between borehole and monitor surface L , equivalent apertures δ , and diffusion parameters k^* .

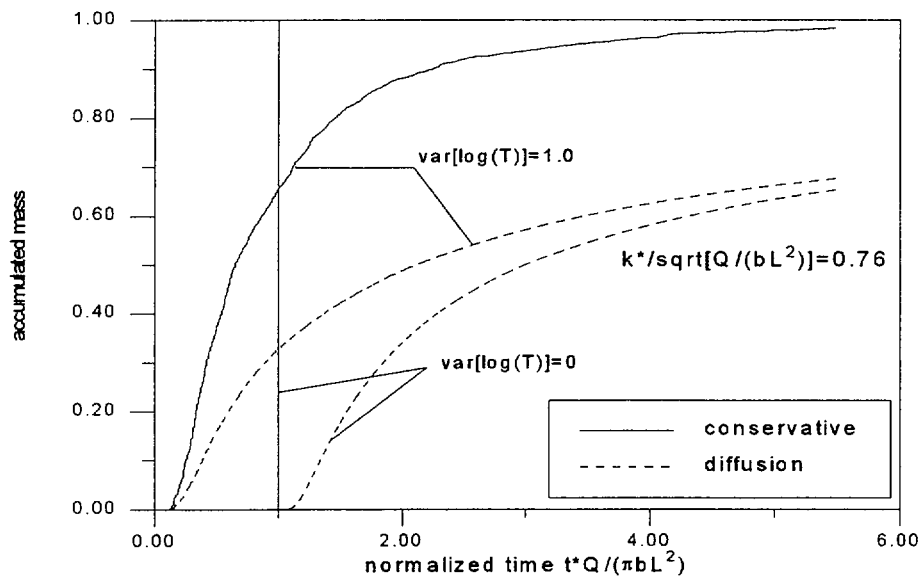


Figure 5-2. Comparison between conservative and diffusion affected cumulative breakthroughs for homogeneous and heterogeneous flow conditions.

For the results presented in Figure 5-2 an equivalent aperture value has been used. If, however, a correlation is assumed to exist between the travel time and aperture distributions the methodology outlined in section 2.4 can be used to incorporate this feature. For the pumping conditions assumed for the MDE the tailing in breakthrough of a conservative solute is a pure result of heterogeneity in transmissivity. Consequently, a correlation can be hypothesized between the travel time and aperture, or between the travel time and the diffusion parameter k^* .

In Figure 5-3 the effect of positive and negative correlation between the travel time and k^* are shown using equation (8) and (9). The specific values of the moments of the log-normal distribution are chosen for illustrative purposes and do not represent the pumping conditions considered previously. It may furthermore be noted that a dimensionless time, defined as real time multiplied with the mean velocity and divided by the integral scale of the log-transmissivity, is used in the presentation of the results. For the MDE-pumping case the travel time is directly proportional to the aperture whereas k^* is inversely proportional to the aperture. Thus the correlation between travel time and k^* is negative; furthermore, the coefficient of variation should be of the same order of magnitude for both the travel time and k^* moments.

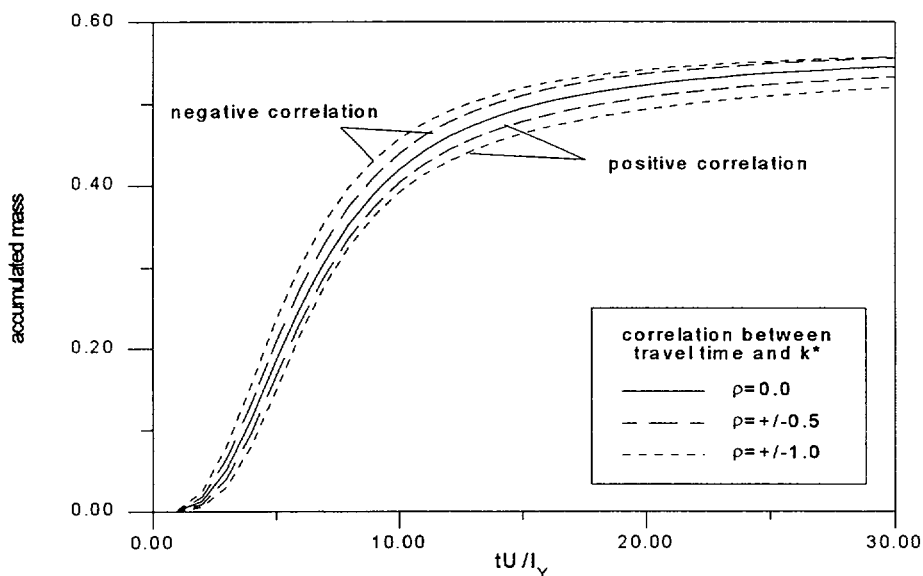


Figure 5-3. Effect of correlation between k^* and τ on the cumulative breakthroughs. The following moments are used in the lognormal distribution:

$$m_{\tau} = 5.0, \sigma_{\tau}^2 = 10, m_{k^*} = 0.1, \sigma_{k^*}^2 = 2.5 \times 10^{-3}$$

It can be seen in Figure 5-3 that the effect of correlation is moderate. Moreover, for negative correlation the breakthrough is somewhat earlier in time than the uncorrelated or positively correlated cases.

The practical use of equation (8) is limited by the fact that the form of the joint pdf has to be assumed. A log normal distribution does not reflect the full features of a pumping affected breakthrough. Moreover, the double integration in (8) is computationally more demanding than the single one in (3). Hence it is of interest to evaluate an effective k^* -value so that the single integration over the pdf in (3) can be used; however, this effective value should reflect the spatial variability of k^* .

In Figure 5-4 a comparison is made between the zero correlation case of Figure 5-3 and three different cases where an effective (and hence uncorrelated) aperture value is used in the single integration over the pdf of travel time. The pdf is assumed to be log-normal with the same moments of travel time as in Figure 5-3. The effective aperture values compared are the arithmetic, geometric and harmonic mean values of k^* . As can be observed in Figure 5-4, the harmonic mean most closely resembles the case with spatial variability in k^* . The other two effective mean values yield earlier breakthroughs.

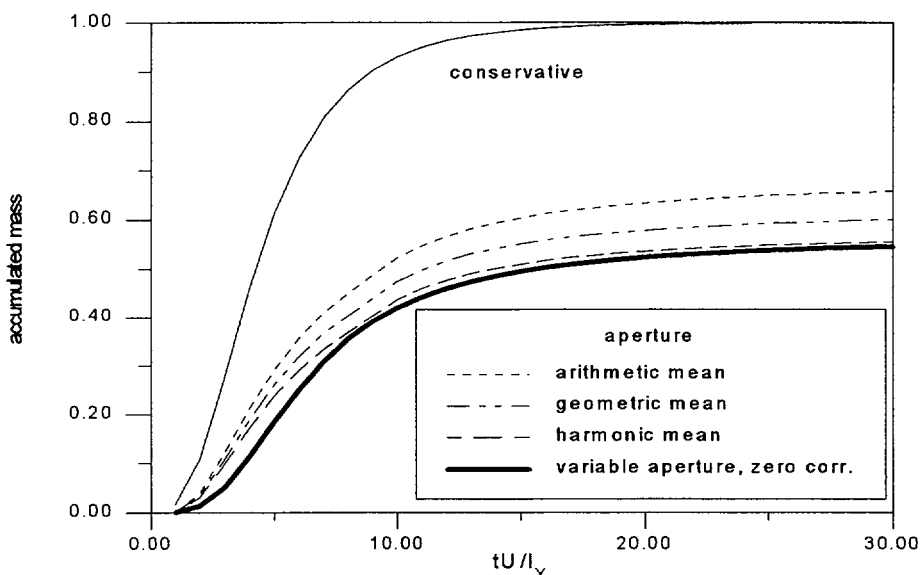


Figure 5-4. Comparison between different effective (mean) values of k^* and a case with variable k^* (zero correlation).

5.3

CONCLUSIONS

The obtained results for the MDE indicate that matrix diffusion may be an active process in the retardation of an advecting solute.

Moreover, the results indicate that spatial variability in the diffusion parameter k^* may have an effect on the mass flux of an advecting tracer. However, the solution is fairly insensitive to the assumed form of correlation (positive or negative, Figure 5-3). More importantly, the effect of spatial variability in the diffusion parameter can be incorporated into a model where variability in k^* is not explicitly addressed (equation (3)) utilizing an effective k^* -value equal to the harmonic mean (Figure 5-4).

The conclusions listed in section 4.3 are to a certain extent valid also for the MDE. Specifically, tailing in breakthrough may be a result of several processes such as heterogeneity in transmissivity and rate-limited mass transfer reactions. However, for the MDE the chosen injection scheme does not induce additional spreading. Finally it should be noted that equilibrium surface sorption has not been included in the simulations. The effect of surface sorption would not, however, modify the qualitative aspects of the obtained results.

DESIGN CONSTRAINTS

In this chapter some practical design constraints and concluding remarks on the two experiments are given. In 6.1 the MWTE is discussed, in 6.2 a corresponding discussion is given for the MDE.

6.1

MULTIPLE WELL TRACER EXPERIMENT

It is impossible to select a fracture for the MWTE with an à priori given transmissivity and aperture distribution. Instead, it will be an iterative process of first identifying and characterizing a fracture and then judging if the fracture may serve for the experimental purposes. Thus, the experimental scheme will greatly benefit from a certain amount of flexibility. The results given in chapter 4, in nomogram form, possess exactly this flexibility. For a given transmissivity (aperture) statistics it may be analyzed with the aid of the nomogram what distances and pumping rates are permissible in order to either experience or avoid rate-limited mass transfer phenomena.

As pointed out in the conclusions of chapter 4, the process discrimination for the MWTE will be quite a formidable task. Three major processes will contribute to the spreading of mass; these are the *dipole pumping scheme*, *heterogeneity in transmissivity* and *various mass transfer processes*. In order to avoid pumping effects different borehole layouts can be imagined such as rows of injection and withdrawal boreholes where a more parallel flow field would result. However, such a scheme would diminish the flexibility of performing the tracer test in different, e.g. perpendicular, directions. Furthermore, the characteristic length scale of the fracture will probably be on the order of a few meters; thus there is a limitation on how many boreholes that can be introduced without significantly altering the hydraulic properties of the fracture. If dipole tracer tests in different directions and over different distances is used it is crucial that the spreading and loss of mass due to the dipole pumping conditions are accounted for.

In order to be able to distinguish between mass spreading resulting from spatial variability in transmissivity and spreading resulting from mass transfer processes it is necessary to work with several tracers. One of these tracers should be truly inert, i.e. completely non-reactive in all respects, the other tracers should have varying sorption (surface and volume) characteristics. However, the equilibrium surface

sorption retardation factor should not exceed 100 in order to be able to perform the experiments during realistic time frames. Furthermore, in order to guarantee identical hydraulic conditions for the different tracers they should be injected simultaneously into the fracture, i.e. a mixture of tracers should be used. However, it is important that the different tracers do not react with each other or compete for e.g. sorption sites on the rock surface or in the rock matrix. It is finally emphasized that the effect of rate-limited mass transfer to a certain extent can be controlled through the selection of pumping rates (section 4.3).

6.2

MATRIX DIFFUSION EXPERIMENT

The general design constraints given in 6.1 for the MWTE are to a certain extent also valid for the MDE. Thus, the presented nomograms may serve as flexible tools once a fracture with given properties has been selected. The major difference between the MWTE and MDE in the scoping calculations performed here is the borehole layout. In the MDE, with only one centrally located borehole, no spreading of mass at the monitor location will result from the pumping. The spreading mechanisms to be considered are only spatial variability in transmissivity and rate-limited mass transfer. The discussion on tracers for the MWTE above also apply for the MDE.

The experimental plan for the MDE /Olsson, 1992/ stipulates that strongly sorbing tracers should be used and that after the finish of the tracer experiment the rock matrix is to be excavated. In our scoping calculations the diffusion front into the matrix has not been explicitly obtained; only the diffusion- and sorption-affected breakthrough in the fracture has been calculated. Thus we would be cautious to suggest any specific experimental conditions for the MDE before further studies have been conducted. However, the conclusions in section 5.3 on the effect of spatial variability in aperture on the diffusion affected breakthrough may have some implications on how to interpret the final results from the MDE.

REFERENES

- Abelin, H. et al 1985: Final Report of the Migration in a Single Fracture - Experimental Results and Evaluation. International OECD/NEA Stripa Project, Stripa Technical Report TR 85-03.
- Abelin, H. et al 1990: Channeling Experiment. International OECD/NEA Stripa Project, Stripa Technical Report TR 90-13.
- Andersson, P. and Klockars, C-E. 1985: Hydrogeological Investigations and Tracer Tests in a Well-defined Rock Mass in the Stripa Mine. Swedish Nuclear Fuel and Waste Management Company, SKB Technical Report SKB TR 85-12.
- Axelsson, C-L. et al. 1989: Discrete Fracture Modelling. Äspö Hard Rock Laboratory Progress Report 25-89-21.
- Brown, D.M. 1984: Stochastic Analysis of Flow and Solute Transport in a Variable-Aperture Rock Fracture. MSc Thesis, MIT, U.S.A.
- Cvetkovic, V. 1991: Mass arrival of reactive solute in single fractures, *Water Resources Research*. vol. 27, pp. 177-183.
- Cvetkovic, V.D. and Shapiro, A.M. 1990: Mass arrival of sorptive solute in heterogeneous porous media, *Water Resources Research*, vol. 26, pp. 2057-2067.
- Derschowitz, W.S., Lee, G., and Geier, J.E. 1991: FracMan Version β 2.3, Interactive Discrete Fracture Data Analysis, Geometric Modelling and Exploration Simulation User Documentation, Report 913-358, Golder Associates Inc., Redmond, Washington, USA.
- Geier, J.E. et al. 1992: Discrete Fracture Modelling of the Finnsjön Rock Mass: Phase 2. Swedish Nuclear Fuel and Waste Management Co, Technical Report TR 92-07.
- Gustafsson, E. and Klockars, C-E. 1981: Studies on Groundwater Transport in Fractured Crystalline Rock under Controlled Conditions using Nonradioactive Tracers. Swedish Nuclear Fuel and Waste Management Company, SKB Technical Report SKB TR 81-07.
- Hakami, E. 1989: Water Flow in Single Rock Joints. International OECD/NEA Stripa Project, Stripa Technical Report TR 89-08.
- Iwai, K. 1976: Fundamental Studies of Fluid Flow through a Single Fracture. PhD Thesis, University of California, Berkeley, CA, U.S.A.
- Lamb, H. 1945: *Hydrodynamics*, Dover Publications, New York,

pp. 69-71.

Lasseby, K.R. 1988: Unidimensional solute transport incorporating equilibrium and rate-limited isotherms with first-order loss, 1, Model conceptualizations and analytic solutions, *Water Resources Research*, vol. 24, pp. 343-350.

Liedholm, M. 1990: Conceptual Modelling of Äspö. Technical note no. 13, Äspö Hard Rock Laboratory Progress Report 25-90-16a.

Mantoglou, A. 1987: Digital simulation of multivariate two- and three-dimensional stochastic processes with a spectral turning bands method, *Mathematical Geology*, vol. 19, pp. 129-150.

Moreno, L., Tsang, Y.W., Tsang, C.F., Hale, F.V. and Neretnieks, I. 1988: Flow and Tracer Transport in a Single Fracture - A Stochastic Model and its Relation to Some Field Observations. *Water Resources Research*, vol. 24, pp. 2033-2048.

Moreno, L., Tsang, C.F., Tsang Y.W. and Neretnieks, I. 1990: Some Anomalous Features of Flow and Solute Transport Arising from Fracture Aperture Variability. *Water Resources Research*, vol. 26, pp. 2377-2391.

Neretnieks, I. 1980: Diffusion in the Rock Matrix: An Important Factor in Radionuclide Retardation? *J. Geophys. Res.*, vol. 85, pp. 4379-4397.

Nordqvist, A.W., Tsang, Y.W., Tsang, C.F., Dverstorp, B. and Andersson, J. 1992: A Variable Aperture Fracture Network Model for Flow and Transport in Fractured Rocks. *Water Resources Research*, vol. 28, pp. 1703-1713.

Olsson, O. 1992: Draft test plan for flow and transport processes in the detailed scale, Release 0.3, December 1992.

Osnes, J.D, Winberg, A., Andersson, J-E. and Larsson, N-Å. 1991: Analysis of Well Test Data - Application of Probabilistic Models to infer Hydraulic Properties of Fractures. Topical Report RSI-0338. DOE/CH/10378-9.

Pyrak-Nolte, L.J. et al 1987: Hydraulic and Mechanical Properties of Natural Fractures in Low Permeability Rock. In Proc. of 6th Int. Congr. on Rock Mech.

Selroos, J.O. and Cvetkovic, V. 1992: Modeling solute advection coupled with sorption kinetics in heterogeneous formations, *Water Resources Research*, vol. 28, pp. 1271-1278.

SKB 1992: Treatment and final disposal of nuclear waste - Äspö Hard Rock Laboratory, Background report to RD&D Programme 92.

Swan, G. 1985: Methods of Roughness Analysis for Predicting Rock Joint Behaviour, Pro. Int. Symp. on Fundamentals of Rock Joints. Björkliden, Sweden, pp. 15-20.

Tomasko, D. 1987: The Effects of a Bimodal Pore Distribution on Matrix Diffusion in a Fractured Porous Medium, Sandia report SAND87-0265, UC-70.

Tsang, Y.W. 1992: Usage of "Equivalent Apertures" for Rock Fractures as Derived from Hydraulic and Tracer Tests. Water Resources Research, vol. 28, pp. 1451-1455.

Tsang, Y.W. and Tsang, C.F. 1987: Channel Model of Flow through Fractured Media. Water Resources Research, vol. 23, pp. 467-479.

Tsang, Y.W. and Tsang, C.F. 1989: Flow Channeling in a Single Fracture as a Two-Dimensional Strongly Heterogeneous Permeable Medium. Water Resources Research, vol. 25, pp. 2076-2080. Technical Note.

Weber, W.J.Jr., McGinley, P.M. and Katz, L.E. 1991: Sorption phenomena in subsurface systems: concepts, models and effects of contaminant fate and transport, Water Resources, vol. 25, pp. 499-528.

Wickberg, P. (ed) et al 1991: Äspö Hard Rock Laboratory. Evaluation and Conceptual Modelling based on the Pre-investigations 1986-1990. Swedish Nuclear Fuel and Waste Management Co, Technical Report TR 91-22.

GROUNDWATER FLOW AND TRANSPORT MODEL	
Numerical-analytical methodology	
Process description Stochastic generation of transmissivity fields Equation of continuity for fluid Darcy's law Kinematic description of particle transport Mass transfer reactions along flow paths	
CONCEPTS	DATA
Geometric framework and parameters	
2 D domain	60×61 square elements in grid
Material properties	
Transmissivity (T)	T obtained using Turning Bands method
Spatial assignment model	
Stochastic assignment of T -values according to exponential covariance function	Mean, variance and correlation length of $\log(T)$ assumed
Boundary conditions	
MWTE: constant head on x boundaries, no flow z boundaries, source/sink (injection/abstraction) in two elements	no data used
MDE: constant head along all boundaries, source (injection) in one element	
Numerical tools	
Transmissivity generation: Turning Bands method (TUBA)	
Flow solver: Finite difference code	
Transport: Particle tracking	
Matrix diffusion/sorption: Numerical integration of equations (3) or (8), c.f. 2.1 and 2.4	
Output parameters	
TUBA: Transmissivity fields	
Flow solver: Hydraulic heads, velocities	
Particle tracking: Breakthrough curves of nonreactive solute mass	
Integration of eq. (3) or (8): Breakthrough curves of reactive solute mass	

List of International Cooperations Reports

ICR 93-01

Flowmeter measurement in
borehole KAS 16
P Rouhiainen
June 1993
Supported by TVO, Finland

ICR 93-02

Development of ROCK-CAD model
for Äspö Hard Rock Laboratory site
Pauli Saksa, Juha Lindh,
Eero Heikkinen
Fintact KY, Helsinki, Finland
December 1993
Supported by TVO, Finland

ICR 93-03

Scoping calculations for the Matrix
Diffusion Experiment
Lars Birgersson¹, Hans Widén¹,
Thomas Ågren¹, Ivars Neretnieks²,
Luis Moreno²
1 Kemakta Konsult AB, Stockholm,
Sweden
2 Royal Institute of Technology,
Stockholm, Sweden
November 1993
Supported by SKB, Sweden

ICR 93-04

Scoping calculations for the Multiple
Well Tracer Experiment - efficient design
for identifying transport processes
Rune Nordqvist, Erik Gustafsson,
Peter Andersson
Geosigma AB, Uppsala, Sweden
December 1993
Supported by SKB, Sweden

ICR 94-01

Scoping calculations for the Multiple
Well Tracer Experiment using a variable
aperture model
Luis Moreno, Ivars Neretnieks
Department of Chemical Engineering
and Technology, Royal Institute of
Technology, Stockholm, Sweden
January 1994
Supported by SKB, Sweden

ICR 94-02

**Äspö Hard Rock Laboratory. Test plan for
ZEDEX - Zone of Excavation Disturbance
EXperiment. Release 1.0**

February 1994

Supported by ANDRA, NIREX, SKB

ICR 94-03

**The Multiple Well Tracer Experiment -
Scoping calculations**

Urban Svensson

Computer-Aided Fluid Engineering

March 1994

Supported by SKB, Sweden

ISSN 1104-3210
ISRN SKB-ICR--94/4--SE
CM Gruppen AB, Bromma 1994